JGP Journal of General Physiology

ARTICLE

cMyBP-C phosphorylation modulates the time-dependent slowing of unloaded shortening in murine skinned myocardium

Jasmine Giles[1], Daniel P. Fitzsimons[2], Jitandrakumar R. Patel[1], Chloe Knudtsen[1], Zander Neuville[1], and Richard L. Moss[1]

In myocardium, phosphorylation of cardiac myosin-binding protein-C (cMyBP-C) is thought to modulate the cooperative activation of the thin filament by binding to myosin and/or actin, thereby regulating the probability of cross-bridge binding to actin. At low levels of Ca^{2+} activation, unloaded shortening velocity (V_o) in permeabilized cardiac muscle is comprised of an initial high-velocity phase and a subsequent low-velocity phase. The velocities in these phases scale with the level of activation, culminating in a single high-velocity phase (V_{max}) at saturating Ca^{2+}. To test the idea that cMyBP-C phosphorylation contributes to the activation dependence of V_o, we measured V_o before and following treatment with protein kinase A (PKA) in skinned trabecula isolated from mice expressing either wild-type cMyBP-C (tWT), nonphosphorylatable cMyBP-C (t3SA), or phosphomimetic cMyBP-C (t3SD). During maximal Ca^{2+} activation, V_{max} was monophasic and not significantly different between the three groups. Although biphasic shortening was observed in all three groups at half-maximal activation under control conditions, the high- and low-velocity phases were faster in the t3SD myocardium compared with values obtained in either tWT or t3SA myocardium. Treatment with PKA significantly accelerated both the high- and low-velocity phases in tWT myocardium but had no effect on V_o in either the t3SD or t3SA myocardium. These results can be explained in terms of a model in which the level of cMyBP-C phosphorylation modulates the extent and rate of cooperative spread of myosin binding to actin.

Introduction

In permeabilized cardiac and skeletal muscle fibers, unloaded shortening velocity (V_o) has been shown to scale with the level of Ca^{2+} activation (Moss, 1986; Hofmann et al., 1991a; Hofmann et al., 1991b; Martyn et al., 1994; Swartz and Moss, 2001; Morris et al., 2003). During maximal Ca^{2+} activation, the time course of unloaded shortening is monophasic and linear in skinned skeletal and cardiac muscle preparations (Hofmann et al., 1991b; Strang et al., 1994) and is thought to manifest the rate of cross-bridge detachment from actin. In contrast, the time course of unloaded shortening during submaximal Ca^{2+} activation is biphasic, exhibiting an initial high-velocity phase and a subsequent low-velocity phase. The molecular basis for the low-velocity phase of V_o has been proposed to involve one or more mechanisms, including a shortening-induced cooperative inactivation of the thin filament (Swartz and Moss, 2001) or possibly an effect of myosin-binding protein-C (MyBP-C), which by binding to both actin and myosin may introduce an activation-dependent internal load that slows V_o at low levels of Ca^{2+} activation (Hofmann et al., 1991b; Previs et al., 2012).

The possible involvement of cardiac MyBP-C (cMyBP-C) in the biphasic shortening observed in cardiac muscle is intriguing, given that cMyBP-C is phosphorylated in response to β-adrenergic stimulation (Sadayappan et al., 2011; Gresham et al., 2017) or increased beat frequency (Tong et al., 2015). PKA-mediated phosphorylation of cMyBP-C has been shown to accelerate the kinetics of cross-bridge cycling during submaximal Ca^{2+} activation (Stelzer et al., 2006; Tong et al., 2008; Gresham et al., 2017), which would contribute to accelerated rates of myocardial force development in response to β_1-agonists (Tong et al., 2015; Mamidi et al., 2017). X-ray diffraction studies have demonstrated that phosphorylation of cMyBP-C or replacement of M-domain phosphoserines with phosphomimetic aspartates (i.e., phosphomimetic cMyBP-C [t3SD]) causes radial displacement of myosin cross-bridges away from the thick filament backbone and reduces interfilament lattice

[1]Department of Cell and Regenerative Biology, University of Wisconsin School of Medicine and Public Health, and the University of Wisconsin Cardiovascular Research Center, Madison, WI; [2]Department of Animal, Veterinary and Food Sciences, College of Agricultural and Life Sciences, University of Idaho, Moscow, ID.

Correspondence to Richard L. Moss: rlmoss@wisc.edu

This work is part of a special collection on myofilament function and disease.

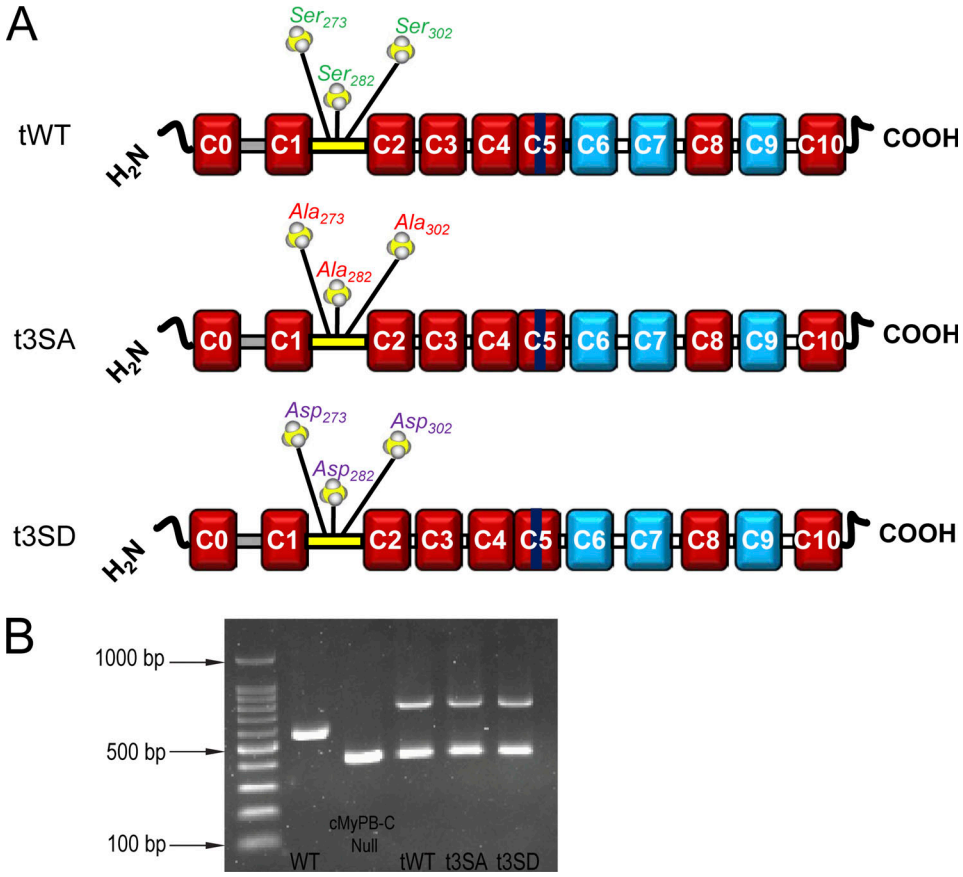

Figure 1. **Generation of mice expressing cMyBP-C. (A)** Diagrammatic representation of the M-domain residues of interest in tWT, t3SA, and t3SD myocardium. **(B)** A PCR genotyping strategy was used to identify the transgenic mice. Shown are PCR products amplified from genomic DNA from WT (cMyBP-$C^{+/+}$), cMyBP-C null (cMyBP-$C^{-/-}$), tWT (cMyBP-$C^{-/-}$, TG-$WT^{+/0}$), t3SA (cMyBP-$C^{-/-}$, TG-$3SA^{+/0}$), and t3SD (cMyBP-$C^{-/-}$, TG-$3SD^{+/0}$) mice.

spacing (Colson et al., 2008; Colson et al., 2012). Shifting cross-bridge mass toward the thin filament would tend to increase the probability of cross-bridge binding to actin and facilitate the cooperative spread of strong cross-bridge binding along the thin filament, thereby accelerating the kinetics of force development.

The present studies were designed to determine the effects of phosphorylation of M-domain phosphoserines (Ser^{273}, Ser^{282}, Ser^{302}) in cMyBP-C on V_o during submaximal levels of Ca^{2+} activation. Our approach was to transgenically express WT cMyBP-C (tWT; Ser^{273}, Ser^{282}, Ser^{302}), nonphosphorylatable cMyBP-C (t3SA; Ala^{273}, Ala^{282}, Ala^{302}), and t3SD (Asp^{273}, Asp^{282}, Asp^{302}) on the cMyBP-C null background (i.e., cMyBP-$C^{-/-}$, $TG^{+/0}$; Fig. 1). We hypothesized that PKA-mediated phosphorylation of the M-domain phosphoserine residues in tWT myocardium or expression of t3SD in myocardium would accelerate the low-velocity phase of unloaded shortening but have no effect on this phase of shortening in myocardium expressing t3SA.

Materials and methods

Mouse models

To determine whether the M-domain phosphoserine residues (Ser^{273}, Ser^{282}, Ser^{302}) contribute to the acceleration of V_o following PKA treatment, we expressed three transgenic forms of cMyBP-C on the cMyBP-C null (cMyBP-$C^{-/-}$) background (Fig. 1): (1) tWT, transgenic expression of WT cMyBP-C (Ser^{273}, Ser^{282}, Ser^{302}); (2) t3SA, transgenic expression of nonphosphorylatable cMyBP-C (Ala^{273}, Ala^{282}, Ala^{302}); and (3) t3SD, transgenic expression of phosphomimetic cMyBP-C (Asp^{273}, Asp^{282}, Asp^{302}; Tong et al., 2008; Colson et al., 2012; Rosas et al., 2015). cMyBP-C–null mice (Harris et al., 2002), WT 129SVE mice (purchased from Taconic Farms), and a non-PKA phosphorylatable cardiac tropinin I mice (in which Ser^{23} and Ser^{24} were substituted with Ala residues ($cTnI_{Ala2}$); Pi et al., 2002) were used as experimental controls before and following PKA treatment. All procedures for animal care, handling, and use were reviewed and approved by the Animal Care and Use Committee of the University of Wisconsin School of Medicine and Public Health.

Steady-state mechanical measurements

Isolation of right ventricular trabeculae

Hearts were rapidly excised from mice of either sex (3–6 mo old) previously injected with 5,000 U heparin/kg body weight and anesthetized with isoflurane. The left and right ventricles were separated at the septum, pinned to the base of a dissecting dish, and perfused with a Ca^{2+}–Ringer's solution (in mM: 120 NaCl, 19 $NaHCO_3$, 5 KCl, 1.2 Na_2HPO_4, 1.2 $MgSO_4$, 1 $CaCl_2$, and 30 2,3-butanedione monoxime, pH 7.4, at 22°C) preequilibrated with 95%

O_2/5% CO_2. After 30 min, the ventricles were rapidly frozen in liquid N_2 and stored at −80°C until used. Permeabilized right ventricular trabeculae were prepared as described previously (Patel, et al., 2012). In brief, the frozen ventricles were thawed in ice-cold relaxing solution (in mM: 100 KCl, 20 imidazole, 4 MgATP, 2 EGTA, and 1 free Mg^{2+}) and then cut open. The exposed trabeculae were dissected free, tied to sticks to hold muscle length (ML) fixed, and transferred to fresh, ice-cold relaxing solution containing 1% Triton X-100 and 0.25 mg/ml saponin. After 60 min, the trabeculae were transferred to fresh, ice-cold relaxing solution and used for mechanical measurements within 2–3 h.

Solutions

Solution compositions were calculated using the computer program of Fabiato (1988), and stability constants (Godt and Lindley, 1982) were corrected to pH 7.0 and 22°C for all solutions. The composition of preactivating solution was (in mM) 100 N,N-Bis(2-hydroxyethyl)-2-aminoethanesulfonic acid (BES), 15 creatine phosphate, 5 dithiothreitol (DTT), 4 MgATP, 1 free Mg^{2+}, and 0.07 EGTA. Activating solution contained (in mM) 100 BES, 15 creatine phosphate, 7 EGTA, 5 DTT, 4 MgATP, and 1 free Mg^{2+}, with $[Ca^{2+}]_{free}$ (pCa) ranging from 1 nM (i.e., pCa 9.0) to 32 µM (i.e., pCa 4.5). A range of submaximal pCa solutions containing different $[Ca^{2+}]_{free}$ were prepared by mixing pCa 9.0 and pCa 4.5 solutions. The ionic strength of the preactivating and activating solutions was adjusted to 180 mM using potassium propionate.

Experimental apparatus

Before each experiment, the ends of a trabecula (400–1,000 µm long × 100–200-µm diameter) were trimmed and mounted between a force transducer (Model 403A; Aurora Scientific) and a high-speed length controller (Model 322C; Aurora Scientific). The experimental apparatus was placed on the stage of an inverted microscope (Model IX70; Olympus) fitted with a 40× objective and a CCTV camera (Model WV-BL600; Panasonic). A halogen lamp was used to illuminate the skinned trabecula. Bitmap images of the trabecula were acquired using an AGP 4X/2X graphics card and associated software (ATI Technologies) and were used to measure mean sarcomere length and fiber dimensions during activation and relaxation. All experiments were performed at 22°C and at a sarcomere length of ∼2.20 µm in pCa 9.0 solution. Changes in force and motor position were sampled (16-bit resolution, DAP5216a; Microstar Laboratories) at 2.0 kHz using SLControl software (http://www.slcontrol.com). All data were saved to computer files for subsequent analysis.

V_o

Prior to measurements of V_o, each trabecula was exposed to solutions of varying pCa (i.e., pCa 6.4–4.5) and allowed to generate steady-state force. The trabecula was then rapidly (<2 ms) slackened by 20% of its original length, resulting in an abrupt reduction of force to near zero, followed by a brief period (15 ms) of unloaded shortening, after which the preparation was restretched rapidly (<2 ms) to its original length and force was allowed to recover. The difference between steady-state force and the force baseline after the 20% slack step was measured as the total force at that pCa. Ca^{2+}-activated force was obtained by subtracting Ca^{2+}-independent force, measured in solution of pCa 9.0, from the total force. Half-maximal Ca^{2+}-activated force (P) was expressed as a fraction of maximal force (P_o) determined at pCa 4.5, i.e., P/P_o, and was used to determine the pCa required for half-maximal activation. Table 1 summarizes the values of maximal total force (P_{Tot}), maximal Ca^{2+}-activated force (P_o), Ca^{2+}-independent force (P_{rest}), maximal rate of force redevelopment, and maximal unloaded shortening velocity (V_{max}). P_{Tot}, P_o, and P_{rest} values were obtained by dividing millinewtons by the cross-sectional area determined using the width of the trabecula. Assessment of preparation dimensions strongly suggests that the difference in P_{Tot} of the t3SA myocardium following PKA treatment is due to differences in width between the control (197.0 ± 23.0 µm) and PKA-treated preparations (157.0 ± 11.4 µm). In experiments assessing the effects of PKA-mediated phosphorylation of cMyBP-C on V_o, trabeculae were incubated before mechanical measurements for 1 h in a solution of pCa 9.0 containing 1 U catalytic subunit of bovine PKA (Sigma) per microliter of pCa 9.0 solution. In each of the WT and mutant lines studied, the experiments were performed in an unpaired manner (i.e., preparations were randomly assigned to either the control group or the PKA-treated group in order to avoid complications due to "run-down" in force over time and during repeated measurements, which is especially problematic with myocardial permeabilized preparations).

The slack test method (Edman, 1979) was used to determine V_o during half-maximal (P/P_o ∼0.5) and maximal levels (P_o) of Ca^{2+} activation (Fig. 2). In brief, once steady-state isometric force was reached, the trabecula was rapidly (<2 ms) slackened starting from a sarcomere length of ∼2.20 µm. Slack steps of varying amplitudes (i.e., 8–20% of its original length) were imposed and held for 500 ms, at which point the trabecula was reextended (Fig. 2). During maximal activation (i.e., measurement of V_{max}), the various length changes were introduced in successive contractions, while in half-maximal activations the preparation was repeatedly slackened and reextended during continuous Ca^{2+} activation. The time from imposition of a slack step to the redevelopment of force was measured by fitting a horizontal line through the force baseline and determining its intersection with a straight line drawn through the initial portion of force redevelopment (Fig. 2). The largest imposed slack was such that the preparation did not shorten below a sarcomere length of 1.80 µm, at which point distortion of velocity due to mechanical restoring forces within the preparation is likely to occur (Strang et al., 1994). Length change was plotted as a function of duration of unloaded shortening. V_o was determined from the slope of the line fitted to the data by linear regression analysis (Fig. 2). V_{max} slack-test data were monophasic and well fitted by a single straight line. V_o slack-test data measured at half-maximal Ca^{2+} activation were biphasic, in which the data were well fitted by two straight lines corresponding to the high-velocity (V_H) and low-velocity (V_L) phases of shortening (Moss, 1986; Swartz and Moss, 2001). Data obtained from a given trabecula were discarded if the regression coefficient was <0.95. Table 2 summarizes the effects of PKA on the V_H and V_L phases of shortening during half-maximal Ca^{2+} activation.

PAGE

Preparation of myofibrillar proteins

Myofibrillar proteins were extracted from tWT, t3SA, and t3SD frozen ventricles (Giles et al., 2019). The frozen ventricles were

Table 1. **Summary of steady-state mechanical measurements**

Measurement	WT (4)	WT (4)	$cTnI_{Ala2}$ (4)	$cTnI_{Ala2}$ (4)	cMyBP-C null (4)	cMyBP-C null (4)
	Basal	(+) PKA	Basal	(+) PKA	Basal	(+) PKA
P_{Tot} (mN mm^{-2})	27.6 ± 7.7	35.4 ± 5.5	26.3 ± 5.6	34.3 ± 8.2	18.9 ± 3.7	35.7 ± 3.8
P_o (mN mm^{-2})	24.1 ± 8.6	33.2 ± 4.8	23.5 ± 4.9	31.0 ± 8.1	16.2 ± 3.1	32.9 ± 3.3
P_{rest} (mN mm^{-2})	3.4 ± 1.1	2.2 ± 0.6	2.7 ± 0.9	3.3 ± 1.3	2.7 ± 0.6	2.8 ± 0.5
k_{tr} (s^{-1})	19.7 ± 1.4	23.2 ± 0.8	19.5 ± 0.9	27.7 ± 3.0	24.4 ± 1.7	31.0 ± 1.5
V_{max} (ML s^{-1})	4.9 ± 0.4	5.4 ± 0.2	4.3 ± 0.4	5.2 ± 0.4	5.3 ± 0.1	5.3 ± 0.2
	tWT (5)	tWT (4)	t3SA (6)	t3SA (6)	t3SD (6)	t3SD (5)
	Basal	(+) PKA	Basal	(+) PKA	Basal	(+) PKA
P_{Tot} (mN mm^{-2})	27.3 ± 6.3	23.8 ± 3.8	18.6 ± 3.3	24.9 ± 1.7	20.8 ± 3.4	15.7 ± 3.2
P_o (mN mm^{-2})	25.1 ± 5.7	22.1 ± 3.4	15.8 ± 3.5	22.3 ± 1.4	19.3 ± 3.3	14.8 ± 3.1
P_{rest} (mN mm^{-2})	2.2 ± 0.5	1.6 ± 0.5	2.7 ± 0.8	2.5 ± 0.6	1.4 ± 0.4	1.0 ± 0.1
k_{tr} (s^{-1})	21.0 ± 1.7	19.5 ± 0.2	23.2 ± 1.8	21.5 ± 1.3	20.8 ± 1.1	21.6 ± 2.9
V_{max} (ML s^{-1})	5.4 ± 0.1	5.5 ± 0.1	5.3 ± 0.3	5.3 ± 0.3	5.6 ± 0.2	5.0 ± 0.3

All values are expressed as mean ± SEM, with the number of trabecular preparations listed in parentheses.
k_{tr}, maximal rate of tension redevelopment at pCa 4.5; P_o, maximal Ca^{2+}-activated tension at pCa 4.5; P_{rest}, Ca^{2+}-independent tension at pCa 9.0; P_{Tot}, maximal Ca^{2+}-activated tension (maximal Ca^{2+}-activated tension plus Ca^{2+}-independent tension); V_{max}, maximal unloaded shortening velocity at pCa 4.5.

pulverized under liquid N_2, homogenized in fresh, ice-cold relaxing solution, and centrifuged. The resulting pellet was resuspended in fresh, ice-cold relaxing solution containing 1% Triton X-100 and 0.25 mg/ml saponin for 30 min at room temperature. After the second centrifugation and wash, the resulting myofibrillar pellet was resuspended in ice-cold relaxing solution, split into two aliquots, and centrifuged. One myofibrillar pellet was solubilized in SDS sample buffer containing 62.5 mM Tris-HCl, 5 mM DTT, 15% glycerol, and 2% SDS, pH 6.8, and stored at −80°C until subsequent analysis. The second myofibrillar pellet was resuspended in ice-cold relaxing solution

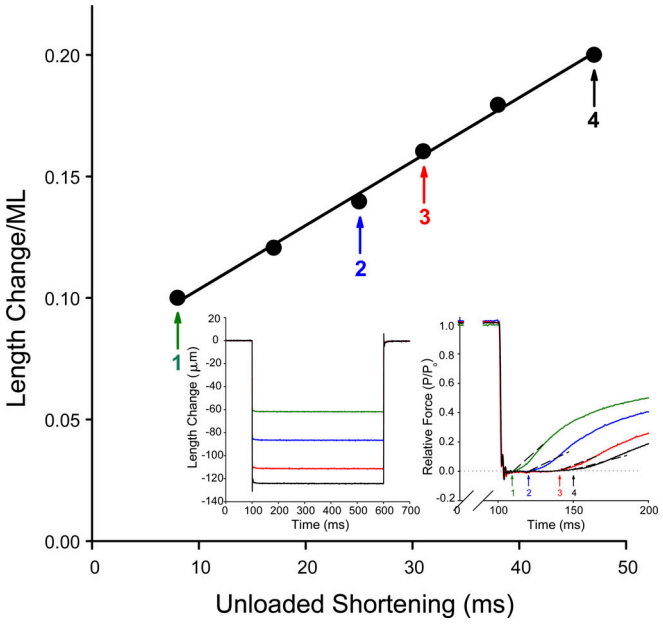

Figure 2. **Experimental protocol for determining V_o.** Inset: Length steps of varying amplitudes (i.e., 8–20% per ML) were imposed and held for 500 ms, followed by rapid reextension. The time from imposition of the slack step to the onset of force redevelopment was measured at the intersection of a horizontal line through the force baseline and a dashed straight line drawn through the initial phase of force redevelopment. Plot: Length change was plotted as a function of time of unloaded shortening, and V_o was obtained from the slope of the line fitted to the data by linear regression analysis.

Table 2. **Effects of PKA on V_o at half-maximal activation**

Animal group	Treatment	P/P_o	V_H (in ML s^{-1})	V_L (in ML s^{-1})
WT	Basal (4)	0.493 ± 0.017	2.0 ± 0.2	1.0 ± 0.1
	PKA (4)	0.551 ± 0.029	2.9 ± 0.2[a]	1.9 ± 0.2[a]
$cTnI_{Ala2}$	Basal (4)	0.585 ± 0.010	2.1 ± 0.2	1.0 ± 0.1
	PKA (4)	0.575 ± 0.010	3.1 ± 0.3[a]	1.8 ± 0.1[a]
cMyBP-C null	Basal (5)	0.558 ± 0.050	4.5 ± 0.2	
	PKA (4)	0.572 ± 0.020	4.3 ± 0.1	
tWT	Basal (5)	0.481 ± 0.038	2.0 ± 0.1	0.9 ± 0.1
	PKA (4)	0.512 ± 0.036	3.5 ± 0.2[a]	1.8 ± 0.2[a]
t3SA	Basal (6)	0.518 ± 0.036	2.2 ± 0.1	1.1 ± 0.1
	PKA (6)	0.526 ± 0.026	1.9 ± 0.2	1.1 ± 0.1
t3SD	Basal (6)	0.540 ± 0.042	3.1 ± 0.2	1.9 ± 0.2
	PKA (5)	0.542 ± 0.052	3.9 ± 0.2[a]	1.9 ± 0.1

All values are expressed as mean ± SEM, with the number of trabecular preparations listed in parentheses.
P/P_o, relative Ca^{2+}-activated force.
[a]Significantly different from basal control.

containing 1 U PKA (Sigma) per microliter. After 1 h at room temperature, the myofibrillar suspension was centrifuged, and the resulting pellet was resuspended in SDS sample buffer and stored at −80°C until subsequent analysis. A BCA Protein Assay (Pierce) was used to determine the myofibrillar protein concentration of each sample immediately before SDS-PAGE.

SDS-PAGE

To determine the relative expression levels of cMyBP-C, myofibrillar proteins were loaded onto AnykD Criterion TGX gels (Bio-Rad), electrophoresed at a constant voltage of 150 V for 90 min at room temperature, and silver stained (Patel et al., 2017). Densitometric analysis was performed using Image Lab software (Bio-Rad), with the intensity ratio of the integrated optical density (IOD) corresponding to the cMyBP-C band relative to the IOD of the α-actinin band calculated to correct for loading and to permit comparisons between samples. To determine the phosphorylation state of myofibrillar proteins in WT, $cTnI_{Ala2}$, tWT, t3SA, and t3SD myocardium following treatment with PKA, myofibrillar proteins were loaded onto AnykD Criterion TGX gels (Bio-Rad), electrophoresed at a constant voltage of 150 V for 90 min at room temperature, and stained with Pro-Diamond (Invitrogen) to detect phosphoproteins and SYPRO Ruby (Invitrogen) to detect total myofibrillar protein (Patel et al., 2012). To avoid any minor differences in protein loading between the WT, $cTnI_{Ala2}$, tWT, t3SA, and t3SD samples, we loaded a range of concentrations per sample on the same gel and then determined the slope of the IOD versus concentration for both the phosphoproteins and myofibrillar proteins (Patel et al., 2012).

Immunohistochemistry

Surgically excised tWT (n = 3), t3SA (n = 3), and t3SD (n = 3) hearts were cannulated and perfused with Ca^{2+}-free Ringer's solution in a Langendorff perfusion setup for 30 min and then subsequently fixed with 10% neutral-buffered formalin for 24 h. Cross-sectional views along the coronal plane were obtained from paraffin-embedded samples sectioned at 5 µm. For immunofluorescence analysis, the sections were deparaffinized, rehydrated, and incubated (1:400 dilution) with a polyclonal antibody raised against cMyBP-C (Harris, et al., 2002) in a humidified chamber at 4°C for 16 h. Immunofluorescent detection of cMyBP-C was performed by using a goat anti-rabbit secondary antibody conjugated to Alexa Fluor 488 (1:10,000 dilution; ThermoFisher) and counterstained with 6′-diamidino-2-phenylindole. All sections were imaged on a Leica SP8 3X STED super-resolution microscope provided by the Optical Imaging Core facility at the University of Wisconsin School of Medicine and Public Health.

Statistics

All data are expressed as means ± SEM. Statistical analyses were performed using either one-way ANOVA followed by the Holm-Sidak post hoc test for multiple comparisons or Student's two-tailed t test for independent samples, with significance for each set at $P < 0.05$.

Results

Biphasic unloaded shortening in WT myocardium

Slack-test data obtained during half-maximal and maximal Ca^{2+} activations in WT, cMyBP-C null, and $cTnI_{Ala2}$ myocardium are shown in Fig. 3. During half-maximal Ca^{2+} activation, WT (n = 5) and $cTnI_{Ala2}$ (n = 5) preparations exhibited a characteristic biphasic response composed of an initial high-velocity phase (WT: 2.0 ± 0.2 ML s^{-1}; $cTnI_{Ala2}$: 2.1 ± 0.2 ML s^{-1}) and a subsequent low-velocity phase (WT: 1.0 ± 0.1 ML s^{-1}; $cTnI_{Ala2}$: 1.0 ± 0.1 ML s^{-1}). The velocities in both the fast and slow phases scaled with the level of Ca^{2+} activation, culminating in a monophasic high-velocity phase (V_{max}) at saturating Ca^{2+} (Table 1). In contrast to results from WT and $cTnI_{Ala2}$ myocardium, we observed a single, high-velocity phase in cMyBP-C–null myocardium under control conditions and also following PKA treatment during half-maximal (basal: 4.5 ± 0.2 ML s^{-1}; PKA: 4.3 ± 0.1 ML s^{-1}) and maximal (basal: 5.3 ± 0.1 ML s^{-1}; PKA: 5.3 ± 0.2 ML s^{-1}) Ca^{2+} activation. The absence of biphasic shortening in cMyBP-C–null myocardium is consistent with previous results in single skeletal muscle fibers in which velocity in the low-velocity phase was progressively increased in proportion as the extent of MyBP-C extraction increased (Hofmann et al., 1991a). The elimination of the low-velocity phase in cMyBP-C–null myocardium supports the idea that cMyBP-C normally acts to slow unloaded shortening during submaximal activation under control conditions.

PKA accelerates biphasic shortening velocities in WT myocardium

It is known that β-adrenergic stimulation accelerates contractile kinetics in living myocardium. PKA-mediated phosphorylation of cMyBP-C may underlie this response by increasing the probability of cross-bridge binding to actin, thereby accelerating cross-bridge cycling kinetics (Mun et al., 2014; Kampourakis et al., 2014). To determine whether cMyBP-C phosphorylation accelerates V_o during half-maximal activation, we measured V_o in WT and $cTnI_{Ala2}$ myocardium following treatment with PKA. Phosphoprotein gel analysis (Fig. 4 A) showed that PKA increased phosphorylation of cMyBP-C and cTnI in WT myocardium, but only cMyBP-C was phosphorylated in $cTnI_{Ala2}$ myocardium (Fig. 4 B). PKA did not affect V_{max} in either WT or $cTnI_{Ala2}$ myocardium (Table 1); however, during half-maximal activation, both the high-velocity (WT: 2.0 ± 0.2 versus 2.9 ± 0.2 ML s^{-1}; $cTnI_{Ala2}$: 2.1 ± 0.2 versus 3.1 ± 0.3 ML s^{-1}) and low-velocity (WT: 1.0 ± 0.1 versus 1.9 ± 0.2 ML s^{-1}; $cTnI_{Ala2}$: 1.0 ± 0.1 versus 1.8 ± 0.1 ML s^{-1}) phases were accelerated by PKA treatment (Fig. 5). Thus, the PKA-induced increase in V_o does not involve phosphorylation of cTnI and is attributable to phosphorylation of cMyBP-C.

Sarcomeric incorporation and transgenic expression of cMyBP-C

Prior to measuring V_o in the transgenic myocardium, it was first necessary to confirm that the transgenic cMyBP-C was appropriately incorporated within the sarcomere. Immunofluorescent labeling of myofibrils with anti–cMyBP-C/Alexa Fluor 488 demonstrated characteristic A-band doublets corresponding to cMyBP-C in tWT, t3SA, and t3SD myocardium (Fig. 6 A).

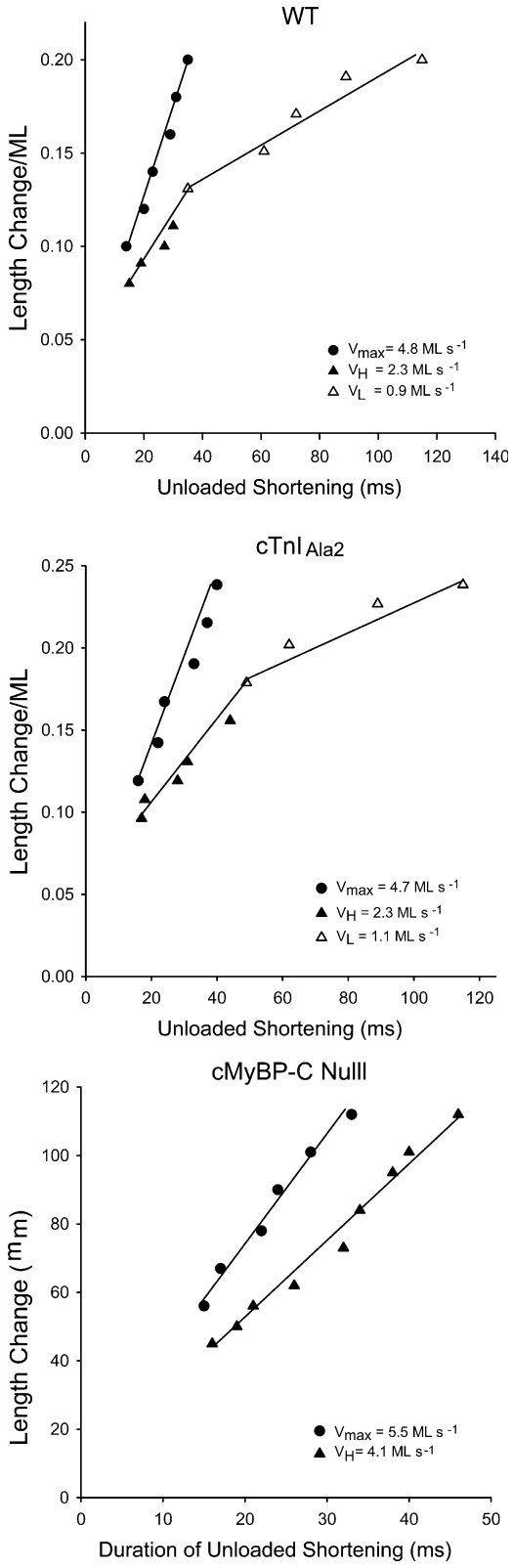

Figure 3. **Slack test data from WT, cTnI$_{Ala2}$, and cMyBP-C–null myocardium.** Representative slack test data were obtained from permeabilized myocardium during half-maximal (V_H: filled triangle; V_L: empty triangle) and maximal (●) Ca^{2+} activations. Ca^{2+}-independent and maximal Ca^{2+}-activated forces were WT (1.7 mN mm^{-2} and 21.1 mN mm^{-2}; preparation length, 550 µm), cTnI$_{Ala2}$ (2.9 mN mm^{-2} and 22.7 mN mm^{-2}; preparation length, 520 µm), and cMyBP-C null (4.2 mN mm^{-2} and 26.0 mN mm^{-2}; preparation length, 560 µm).

SDS-PAGE was performed to ascertain the expression level of transgenic cMyBP-C in tWT, t3SA, and t3SD myocardium. Consistent with previous results (Tong et al., 2008; Colson et al., 2012; Rosas et al., 2015), SDS-PAGE analysis showed similar expression of transgenic cMyBP-C across all three transgenic lines, albeit less than that observed in WT myocardium (i.e., tWT: 72 ± 7%; t3SA: 69 ± 5%; and t3SD: 75 ± 3%; Fig. 6 B). In addition, we determined that the relative expression of α- and β-myosin heavy chain (MyHC) isoforms (expressed as a percentage of total MyHC) was similar in tWT (α: 96.1 ± 0.7%; β: 3.9 ± 0.6%), t3SA (α: 95.7 ± 0.6%; β: 4.3 ± 0.6%), and t3SD (α: 95.4 ± 0.6%; β: 4.6 ± 0.8%) myocardium. From earlier results (Hofmann et al., 1991b), the observed reduction in cMyBP-C expression would be expected to accelerate V_o at half-maximal activation. Since neither the transgenic expression of cMyBP-C nor the expression of MyHC isoforms differed between the three transgenic lines, any differences in V_o before or following PKA treatment can be ascribed to the phosphomimetic replacement or phosphorylation of cMyBP-C, respectively.

V_o in transgenic myocardium

Slack-test data during half-maximal and maximal Ca^{2+} activations were obtained under control conditions in tWT, t3SA, and t3SD myocardium (Fig. 7). During maximal Ca^{2+} activation, V_{max} was monophasic and not significantly different among the three groups (Table 1). Although biphasic shortening was observed in all three groups at half-maximal activation, the respective high- and low-velocity phases were significantly faster in the t3SD (3.1 ± 0.2 ML s^{-1}; 1.8 ± 0.1 ML s^{-1}) myocardium compared with similar values measured in tWT (2.0 ± 0.2 ML s^{-1}; 0.9 ± 0.1 ML s^{-1}) and t3SA (2.1 ± 0.1 ML s^{-1}; 1.1 ± 0.1 ML s^{-1}) myocardium (Fig. 8 B). The greater V_o in the t3SD myocardium under control conditions is likely due to the effects of the near-stoichiometric expression of phosphomimetic aspartate residues, since the basal level of cMyBP-C phosphorylation in the control and two other types of transgenic myocardium were significantly less than stoichiometric (Fig. 8 A).

V_o is accelerated by PKA in tWT myocardium or charge replacement in t3SD myocardium

To determine whether the cMyBP-C M-domain phosphoserine residues are responsible for the greater shortening velocity during half-maximal Ca^{2+} activation, we initially subjected myofibrils isolated from tWT, t3SA, and t3SD myocardium to PKA treatment. As expected, phosphoprotein gels showed that PKA significantly increased cMyBP-C phosphorylation in tWT myocardium (Fig. 8 A). However, neither the nonphosphorylatable nor the phosphomimetic cMyBP-C was significantly phosphorylated in response to PKA treatment, since the Ser-to-Ala and Ser-to-Asp substitutions effectively eliminated the consensus PKA-phosphorylation motifs (i.e., Arg-Arg-X-Ser; Fig. 8 A). PKA treatment significantly increased the level of cTnI phosphorylation in all three transgenic lines to essentially equivalent levels, thereby confirming that PKA activity was similar between experiments (Fig. 8 A).

As predicted from phosphoprotein gel analysis, PKA treatment had no effect on the rates of biphasic shortening in t3SA

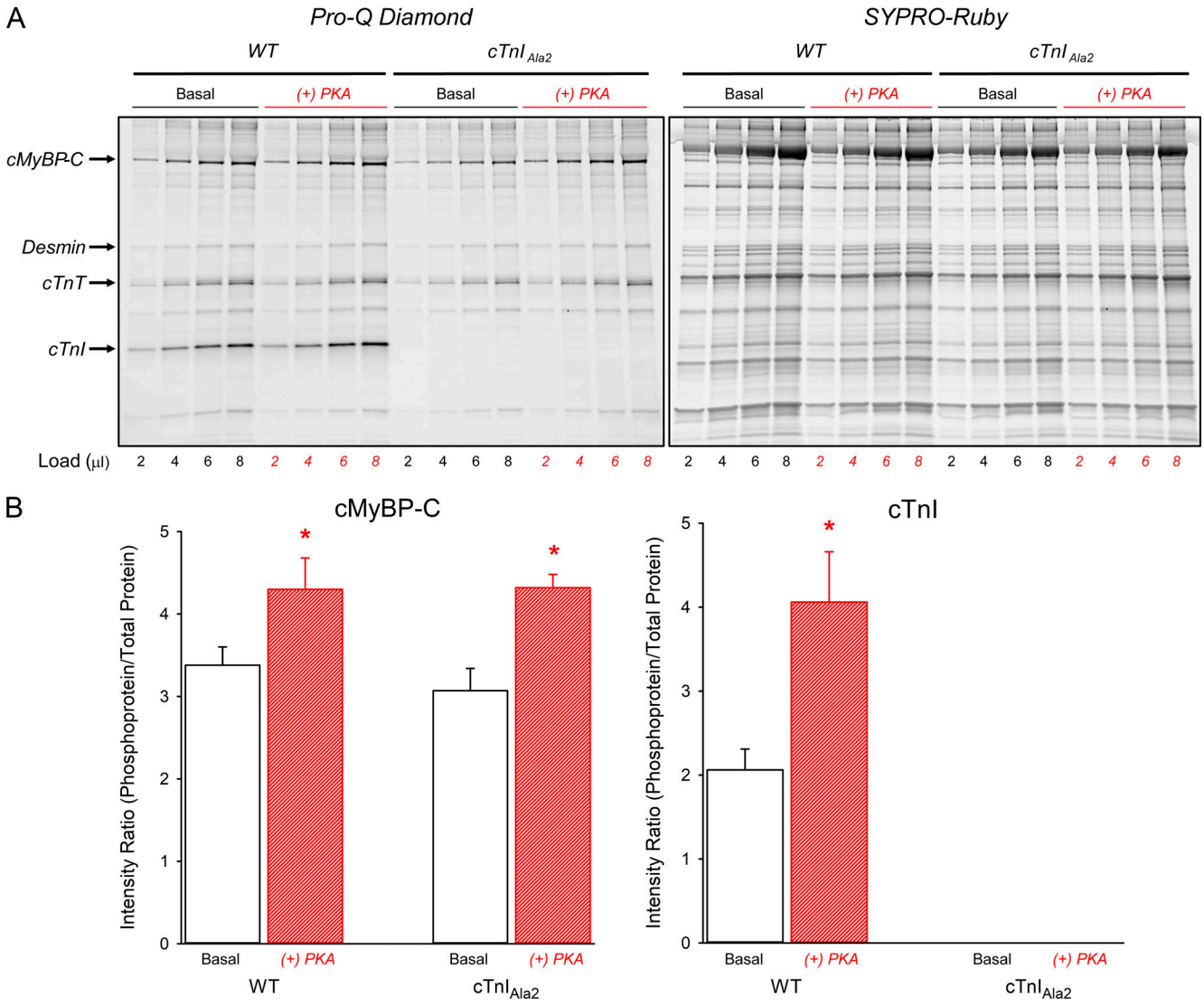

Figure 4. **PKA phosphorylation of cMyBP-C and cTnI in WT and cTnI$_{Ala2}$ myocardium. (A)** Myofibrillar proteins isolated from WT and cTnI$_{Ala2}$ myocardium were separated via SDS-PAGE and then stained with Pro-Q Diamond and SYPRO-Ruby to estimate the levels of cMyBP-C and cTnI phosphorylation under control (basal) conditions and following treatment with PKA. cTnT, cardiac troponin T. **(B)** Relative to control conditions, PKA treatment significantly (*, $P < 0.05$, *t* test) increased the phosphorylation of cMyBP-C and cTnI in WT myocardium but only cMyBP-C in cTnI$_{Ala2}$ myocardium. All values are means ± SEM.

(2.1 ± 0.2 ML s^{-1}; 1.3 ± 0.1 ML s^{-1}) myocardium or the V_L in t3SD (1.8 ± 0.2 ML s^{-1}) myocardium, in that the high- and low-velocity phases did not differ significantly from basal conditions (Fig. 8 B). However, we observed a statistically significant ($P = 0.041$) increase in the V_H after PKA treatment of t3SD myocardium (3.8 ± 0.2 ML s^{-1}), which suggests the possibility that phosphorylation of another residue within cMyBP-C or another myofibrillar protein influences V_o, although this was not evident in the velocity data from PKA-treated cMyBP-C–null myocardium. However, V_o in both the high- and low-velocity phases increased in tWT (3.5 ± 0.3 ML s^{-1}; 1.9 ± 0.2 ML s^{-1}) myocardium following PKA treatment to values similar to those in the t3SD myocardium (Fig. 8 B). Thus, the acceleration of V_o in tWT myocardium requires the phosphorylation or phosphomimetic replacement of phosphoserine residues located within the M-domain of cMyBP-C.

Discussion

cMyBP-C is a thick-filament accessory protein that is readily phosphorylated by PKA in vitro or following β-adrenergic receptor activation in vivo. Phosphoserine residues at positions 273, 282, and 302 have been identified as the primary targets for PKA in the cardiac-isoform of MyBP-C. PKA- (and CaM kinase II–) mediated phosphorylation of cMyBP-C has been proposed to reversibly regulate the interaction of N-terminal domains of cMyBP-C with myosin subfragment-2 (Bhuiyan et al., 2016) and with actin (Bezold et al., 2013; van Dijk et al., 2014) in a phosphorylation-dependent manner (Previs et al., 2016; Kensler et al., 2017). Phosphorylation of cMyBP-C is thought to increase myocardial contractility by disrupting the N-terminal interaction of cMyBP-C with myosin S2, which would effectively increase the rate of cross-bridge binding to actin, and by promoting the interaction of cMyBP-C with actin, thereby

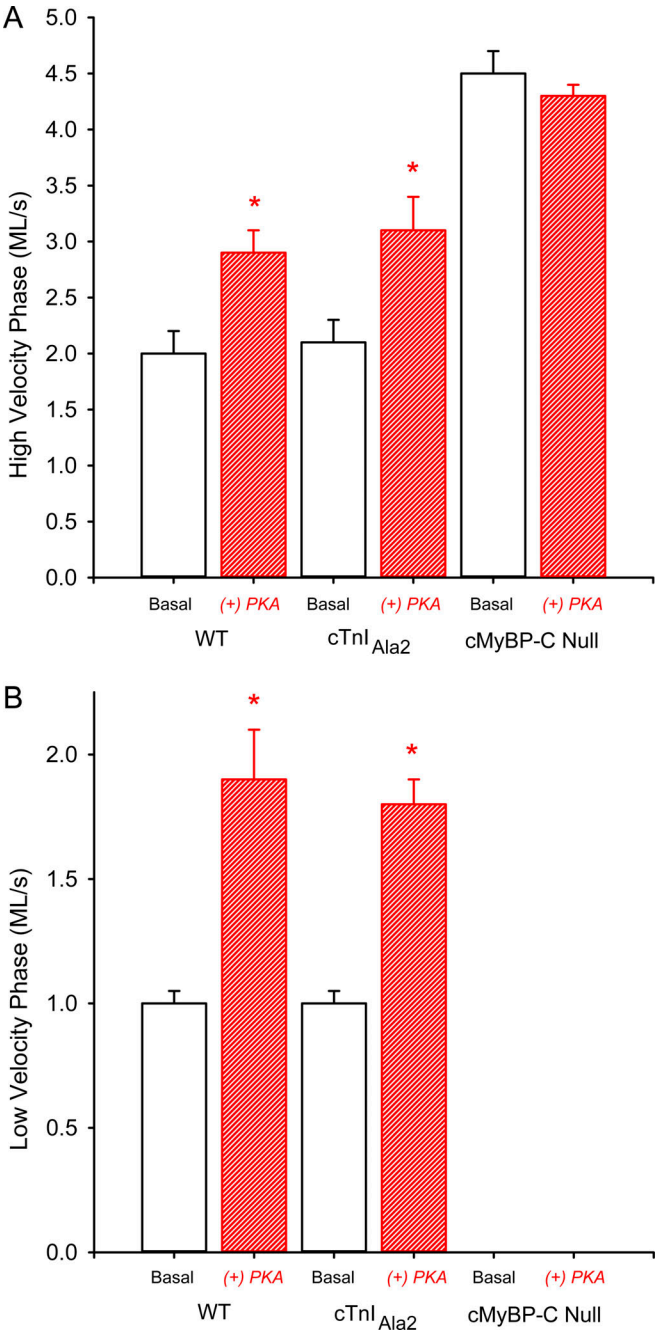

Figure 5. **PKA effects on V_o in WT, $cTnI_{Ala2}$, and cMyBP-C–null myocardium at half-maximal Ca^{2+} activation. (A and B)** Summary data for the high-velocity (A) and low-velocity (B) phases of unloaded shortening in skinned myocardium isolated from WT, $cTnI_{Ala2}$, and cMyBP-C–null myocardium. P/P_o values under control conditions (WT: 0.493 ± 0.017; $cTnI_{Ala2}$: 0.585 ± 0.010) and following PKA treatment (WT: 0.551 ± 0.029; $cTnI_{Ala2}$: 0.575 ± 0.010). All values are means ± SEM; n = 5 hearts/group. PKA treatment significantly (*, $P < 0.05$, t test) increased the velocity of shortening in WT and $cTnI_{Ala2}$ myocardium.

enhancing the activation of the thin filament (Mun et al., 2014; Kampourakis et al., 2014).

Since myocardial shortening velocity is slowed at submaximal Ca^{2+} concentrations corresponding to levels reached in the cardiac twitch, we undertook the present study to determine whether PKA phosphorylation of cMyBP-C would have an effect on shortening velocity, presumably to increase the speed of shortening. Our primary observations are that PKA treatment of permeabilized WT myocardium increased shortening velocity in the V_L and to a much lower degree during the V_H. The effect of PKA to speed the low-velocity phase appears to be due solely to the phosphorylation of cMyBP-C, since myocardium expressing t3SA, in which serine targets of PKA were replaced with alanines, showed no increase in velocity in the low-velocity phase. Importantly, in this experiment there was a significant increase in PKA-mediated phosphorylation of cTnI, but the lack of effect on shortening velocity in the low-velocity phase indicates that increases in cTnI phosphorylation do not account for the effect of PKA on increasing low-velocity shortening in WT myocardium.

Complementary experiments were done to further test these ideas, resulting in a confirmation of our conclusions that phosphorylation of cMyBP-C is the primary mediator of the PKA effects on V_o. In one series of experiments, myocardium expressing tWT and nonphosphorylatable $cTnI_{Ala2}$ showed a robust increase in the V_L in response to PKA. In further experiments, myocardium expressing t3SD exhibited shortening velocities in the V_L that were similar to the velocities observed in WT myocardium treated with PKA.

Before performing the mechanical measurements in transgenic myocardium, we established that the tWT, t3SA, and t3SD lines exhibited (1) equivalent levels of transgenic expression of cMyBP-C and (2) similar patterns of α- and β-MyHC isoform expression. The importance of this determination is emphasized by our observation that there was a single V_H in cMyBP-C–null myocardium during half-maximal Ca^{2+} activation (Fig. 3); that is, the low-velocity phase of V_o was absent. Since the ablation of cMyBP-C eliminates the V_L, differential expression of cMyBP-C in the three transgenic models studied here would by itself be expected to influence V_o even in tWT myocardium. To eliminate this possibility, we selected tWT, t3SA, and t3SD mouse lines exhibiting similar levels of transgenic expression of cMyBP-C (Fig. 6), as also reported previously (Tong et al., 2008; Colson et al., 2012; Rosas et al., 2015). Furthermore, the relative expression of α- and β-MyHC isoforms was similar among the three transgenic models (Fig. 6).

Prior to treatment with PKA, myocardium from all three transgenic lines exhibited biphasic shortening during half-maximal Ca^{2+} activation (Fig. 7). tWT and t3SA myocardium exhibited similar rates of high- and low-velocity shortening, which were significantly slower than that of t3SD myocardium (Fig. 8 B). The higher velocity of shortening in t3SD myocardium is associated with redistribution of cross-bridge mass toward the thin filament, shown previously (Colson et al., 2012), and is presumably a consequence of reduced binding of cMyBP-C to myosin, increased binding to actin, or both. Phosphoprotein gel analysis showed similar levels of basal cMyBP-C phosphorylation in the three lines before PKA treatment (Fig. 8 A). Although the Ser-to-Ala and Ser-to-Asp substitutions would eliminate three consensus PKA motifs in the M-domain, there are additional potential phosphorylation sites in cMyBP-C (Rosas et al., 2015), including a novel phosphorylatable serine residue within the M-domain (Jia et al., 2010), which presumably accounts for

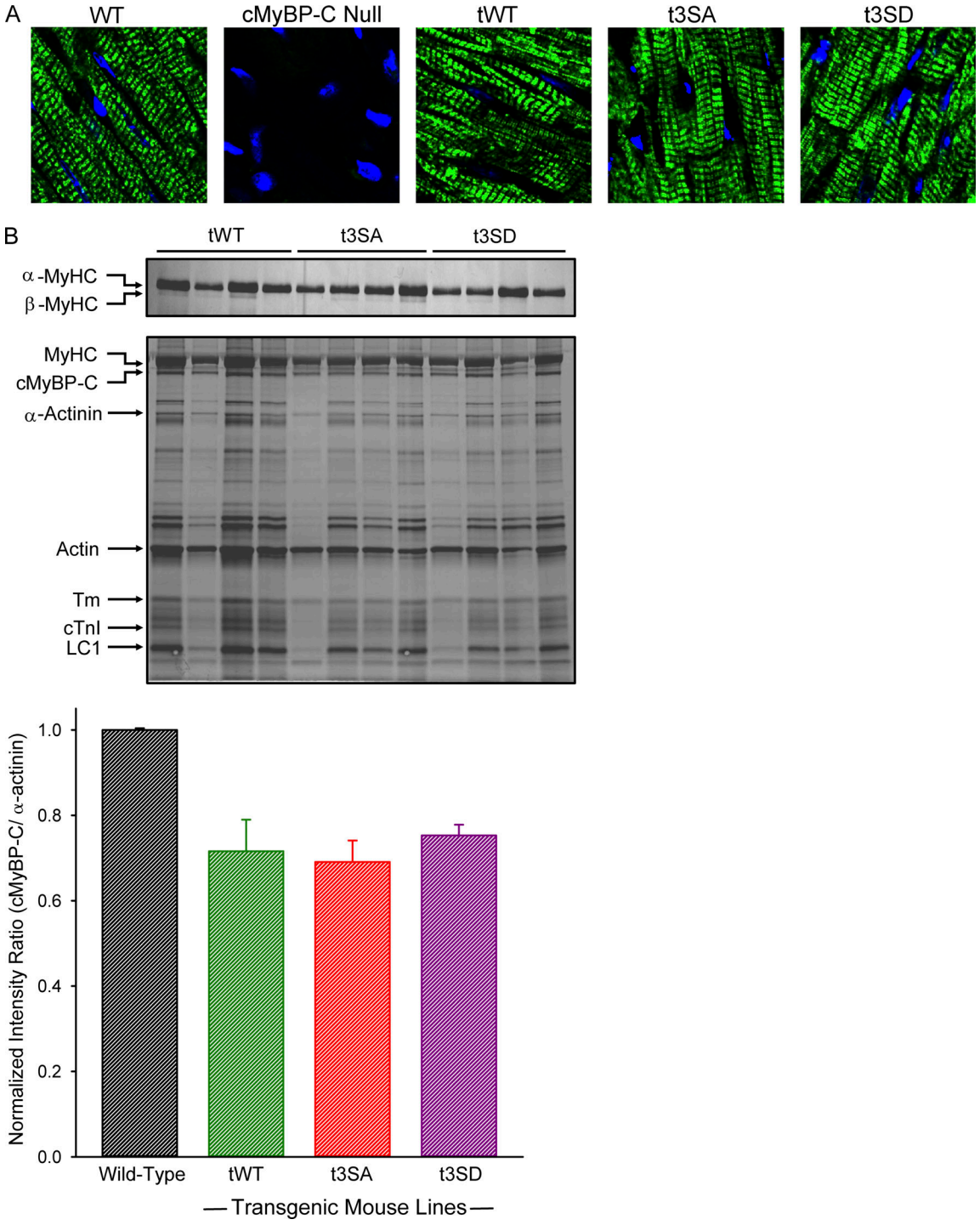

Figure 6. **Incorporation of cMyBP-C in tWT, t3SA, and t3SD myocardium. (A)** Confocal images of WT, tWT, t3SA, and t3SD myocardium. cMyBP-C–null myocardium is included as a negative control. **(B)** SDS-PAGE of tWT, t3SA, and t3SD myofibrils was used to estimate expression of cMyBP-C. Top: Myosin heavy chain isoform expression. Middle: myofibrillar contractile protein expression. Tm, tropomyosin. Bottom: Densitometric analysis of the expression of cMyBP-C relative to α-actinin (intensity ratio). All values are means ± SEM; *n* = 5 hearts/group.

basal phosphorylation in t3SA and t3SD myocardium. However, PKA did not alter the phosphorylation profiles of cMyBP-C in t3SA and t3SD myocardium, and there were no changes in the velocity of unloaded shortening in either of these two lines following PKA treatment (Fig. 8 B). In contrast, PKA had a pronounced effect in tWT myocardium in increasing cMyBP-C phosphorylation (Fig. 8 A) and accelerating V_o (Fig. 8 B). V_o in the V_H and V_L following PKA treatment was essentially the same as the values observed in t3SD myocardium before and after PKA treatment. These data strongly suggest that Ser^{273}, Ser^{282}, and Ser^{302} in cMyBP-C are key residues in the modulation of myocardial contractility in response to variations in β-adrenergic

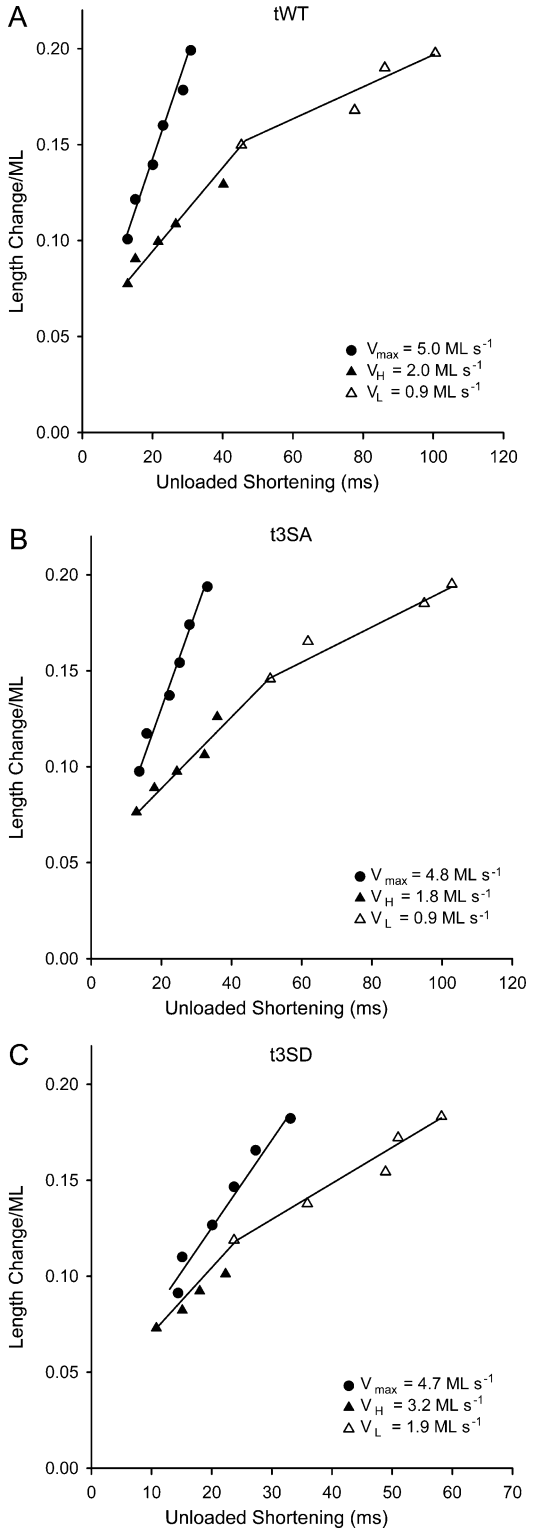

Figure 7. **Slack test data from tWT, t3SA, and t3SD myocardium during submaximal and maximal Ca^{2+} activations. (A–C)** Representative slack test data were obtained from permeabilized tWT (A), t3SA (B), and t3SD (C) myocardium during half-maximal (V_H: full triangle; V_L: empty triangle) and maximal (●) Ca^{2+} activations. Ca^{2+}-independent and maximal Ca^{2+}-activated forces were tWT (1.2 mN mm^{-2} and 28.1 mN mm^{-2}; preparation length, 430 µm), t3SA (4.3 mN mm^{-2} and 28.3 mN mm^{-2}; preparation length, 450 µm), and t3SD (3.3 mN mm^{-2} and 24.0 mN mm^{-2}; preparation length, 500 µm).

inputs to the heart (Sadayappan et al., 2011; Mun et al., 2014; Kampourakis et al., 2014; Gresham et al., 2017).

Possible mechanisms of the effects of cMyBP-C phosphorylation on V_o

Unloaded shortening velocity measured in the presence of saturating Ca^{2+} (V_{max}) is thought to be determined by the rate of ADP release from the myosin–actin complex at the end of the cross-bridge power stroke (Gordon et al., 2000 and references therein). In this and previous studies (Moss, 1986; Hofmann et al., 1991a; Hofmann et al., 1991b; Martyn et al., 1994; Swartz and Moss, 2001; Morris et al., 2003), V_o was observed to decrease as Ca^{2+} concentration was lowered, and the time course of shortening became biphasic, being composed of an initial high-velocity phase and a subsequent low-velocity phase. Changes in Ca^{2+} concentration per se would not be expected to change the rate of ADP release, as was demonstrated previously in solutions containing myosin and regulated thin filaments (Lu et al., 2001). Thus, direct Ca^{2+} regulation of cross-bridge detachment is unlikely to be the basis for the reduced velocities of shortening observed here when Ca^{2+} concentration was lowered or following a period of high-velocity shortening during half-maximal activation. Instead, it seems plausible that one or both phenomena are due to mechanical constraints that either slow the rate of cross-bridge detachment or impede the relative sliding of thick and thin filaments during shortening. Earlier studies have suggested several factors that might give rise to the low-velocity phase of unloaded shortening at submaximal Ca^{2+} concentrations. One proposal is that low-velocity shortening is due to shortening-induced cooperative inactivation of the thin filament, in which the number of cross-bridges strongly bound to actin decreases as shortening proceeds (Iwamoto, 1998; Swartz and Moss, 2001). Since both Ca^{2+} and strongly bound cross-bridges are needed to fully activate the thin filament (Lehrer, 1994; McKillop and Geeves, 1993; Swartz et al., 1996), the combination of low levels of Ca^{2+} and the detachment of cross-bridges as shortening proceeds would reduce the activation state of the thin filament regulatory strand and slow the kinetics of cross-bridge detachment. The finding that NEM-S1, a strong-binding myosin derivative, eliminated the V_L during half-maximal Ca^{2+} activation provides support for this idea (Swartz and Moss, 2001). Slower rates of cross-bridge detachment would presumably introduce an internal load opposing shortening when cross-bridges that have completed a power stroke remain attached to the thin filament. Alternatively, it has been suggested that cooperative deactivation represents an increase in detachment rates of the remaining bound cross-bridges (Hanft et al., 2008). While we are unable to distinguish between these mechanisms, the alternative suggested by Hanft et al. (2008) would not predict the slowing of V_o we observed at submaximal Ca^{2+} activation as shortening proceeds. The low-velocity phase of unloaded shortening might also arise as a consequence of the binding of cMyBP-C simultaneously to both myosin and actin, which would give rise to a resistive internal load as shortening proceeds (Hofmann et al., 1991b; Previs et al., 2012). Possible involvement of MyBP-C in the V_L was suggested by the finding that partial extraction of MyBP-C from

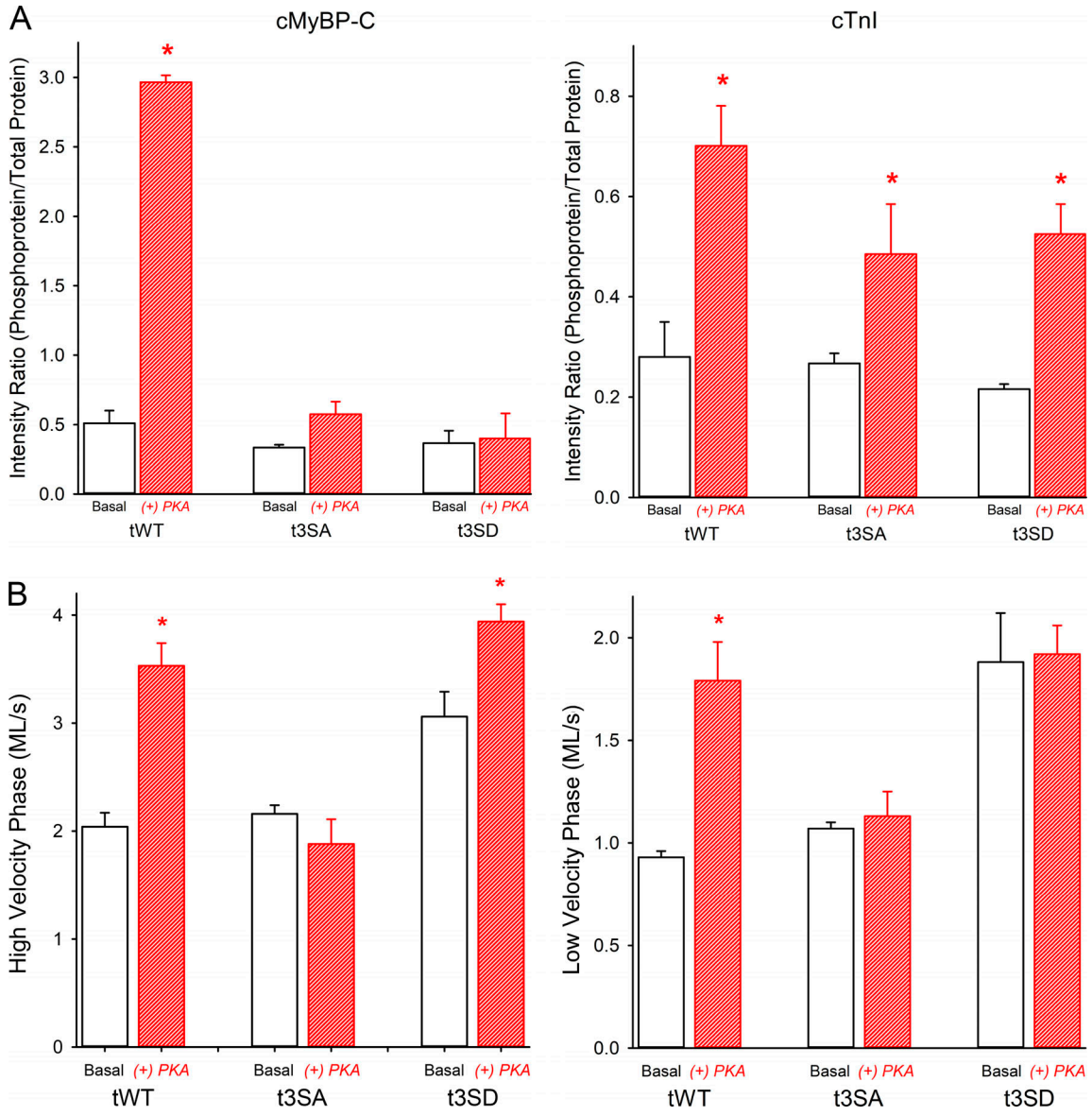

Figure 8. **Effects of PKA phosphorylation of cMyBP-C on V_o in tWT, t3SA, and t3SD myocardium. (A)** PKA phosphorylation of cMyBP-C in tWT, t3SA, and t3SD myocardium. Compared with basal conditions, PKA significantly (*, P < 0.05) increased the phosphorylation of cMyBP-C and cTnI in tWT myocardium but only the phosphorylation of cTnI in t3SA and t3SD myocardium (*, P < 0.05). All values are means ± SEM; *n* = 5 hearts/group. **(B)** PKA phosphorylation increased shortening velocity in the high and low velocity phases only in tWT myocardium. P/P_o values control conditions (tWT: 0.481 ± 0.038; t3SA: 0.518 ± 0.036; t3SD: 0.540 ± 0.042) and following PKA treatment (tWT: 0.512 ± 0.036; t3SA: 0.526 ± 0.026; t3SD: 0.542 ± 0.052). All values are means ± SEM; *n* = 5 hearts/group; *, P < 0.05 indicates significant increases in shortening velocity due to PKA treatment compared with basal conditions.

permeabilized skeletal muscle fibers reversibly increased V_o in the low-velocity phase (Hofmann et al., 1991b). However, in isolation, such a mechanism is difficult to reconcile with the observation that shortening at Ca^{2+} concentrations that yield maximum activation is monophasic, occurs at V_{max}, and is affected by phosphorylation of cMyBP-C.

The observation in the present study that PKA phosphorylation of cMyBP-C increased V_o in the low-velocity phase suggests additional mechanisms suggested by this and previous studies. For example, t3SA has been proposed to stabilize the super-relaxed state of myosin cross-bridges, thereby reducing the probability of cross-bridge binding to the thin filament (McNamara et al., 2016; Hooijman et al., 2011; McNamara et al., 2019). Consistent with this observation, phosphorylation has been shown to disrupt cMyBP-C binding to myosin (Bhuiyan et al., 2016), increase cross-bridge disorder in thick filaments (Kensler et al., 2017), increase the proximity of cross-bridge mass to the thin filaments (Colson et al., 2008; Colson et al., 2012), and increase the activation state of the thin filament (Mun et al., 2014; Kampourakis et al., 2014).

From these observations, phosphorylation of cMyBP-C or insertion of charge-mimetic aspartates in place of M-domain phosphoserines (i.e., t3SD) would be predicted to weaken the binding of cMyBP-C to myosin, resulting in an increased availability of myosin heads and of the N-terminal domain of cMyBP-C for interactions

with actin. Increased binding of myosin heads would cooperatively activate the thin filament, as would binding of cMyBP-C (Harris et al., 2016; Risi et al., 2018; Inchingolo et al., 2019), which has been shown to displace the thin filament regulatory strand toward positions associated with greater activation (Mun et al., 2014). While phosphorylation of cMyBP-C or charge replacement of the M-domain serine residues may ultimately act through different mechanisms (Kampourakis et al., 2018), the net effect of either would be to increase the number of cross-bridges strongly bound to actin, accelerate the kinetics of cross-bridge interaction with actin (Weith et al., 2012; McNamara et al., 2019), and thereby sustain the activation state of the thin filament and the constancy of shortening velocity as shortening proceeds.

Acknowledgments

Henk L. Granzier served as editor.

This work was supported by National Institutes of Health grant RO1 HL139883 to R.L. Moss.

The authors declare no competing financial interest.

Author contributions: D.P. Fitzsimons and R.L. Moss designed the study. J. Giles, J.R. Patel, C. Knudtsen, and Z. Neuville collected the data. J.Giles, D.P. Fitzsimons, and J.R. Patel analyzed the data. D.P. Fitzsimons and R.L. Moss wrote the manuscript, and all authors reviewed the manuscript.

Submitted: 30 September 2020
Accepted: 14 January 2021

References

Bezold, K.L., J.F. Shaffer, J.K. Khosa, E.R. Hoye, and S.P. Harris. 2013. A gain-of-function mutation in the M-domain of cardiac myosin-binding protein-C increases binding to actin. *J. Biol. Chem.* 288:21496–21505. https://doi.org/10.1074/jbc.M113.474346

Bhuiyan, M.S., P. McLendon, J. James, H. Osinska, J. Gulick, B. Bhandary, J.N. Lorenz, and J. Robbins. 2016. In vivo definition of cardiac myosin-binding protein C's critical interactions with myosin. *Pflugers Arch.* 468:1685–1695. https://doi.org/10.1007/s00424-016-1873-y

Colson, B.A., T. Bekyarova, M.R. Locher, D.P. Fitzsimons, T.C. Irving, and R.L. Moss. 2008. Protein kinase A-mediated phosphorylation of cMyBP-C increases proximity of myosin heads to actin in resting myocardium. *Circ. Res.* 103:244–251. https://doi.org/10.1161/CIRCRESAHA.108.178996

Colson, B.A., J.R. Patel, P.P. Chen, T. Bekyarova, M.I. Abdalla, C.W. Tong, D.P. Fitzsimons, T.C. Irving, and R.L. Moss. 2012. Myosin binding protein-C phosphorylation is the principal mediator of protein kinase A effects on thick filament structure in myocardium. *J. Mol. Cell. Cardiol.* 53:609–616. https://doi.org/10.1016/j.yjmcc.2012.07.012

Edman, K.A.P. 1979. The velocity of unloaded shortening and its relation to sarcomere length and isometric force in vertebrate muscle fibres. *J. Physiol.* 291:143–159. https://doi.org/10.1113/jphysiol.1979.sp012804

Fabiato, A. 1988. Computer programs for calculating total from specified free or free from specified total ionic concentrations in aqueous solutions containing multiple metals and ligands. *Methods Enzymol.* 157:378–417. https://doi.org/10.1016/0076-6879(88)57093-3

Giles, J., J.R. Patel, A. Miller, E. Iverson, D. Fitzsimons, and R.L. Moss. 2019. Recovery of left ventricular function following in vivo reexpression of cardiac myosin binding protein C. *J. Gen. Physiol.* 151:77–89. https://doi.org/10.1085/jgp.201812238

Godt, R.E., and B.D. Lindley. 1982. Influence of temperature upon contractile activation and isometric force production in mechanically skinned muscle fibers of the frog. *J. Gen. Physiol.* 80:279–297. https://doi.org/10.1085/jgp.80.2.279

Gordon, A.M., E. Homsher, and M. Regnier. 2000. Regulation of contraction in striated muscle. *Physiol. Rev.* 80:853–924. https://doi.org/10.1152/physrev.2000.80.2.853

Gresham, K.S., R. Mamidi, J. Li, H. Kwak, and J.E. Stelzer. 2017. Sarcomeric protein modification during adrenergic stress enhances cross-bridge kinetics and cardiac output. *J Appl Physiol (1985).* 122:520–530. https://doi.org/10.1152/japplphysiol.00306.2016

Hanft, L.M., F.S. Korte, and K.S. McDonald. 2008. Cardiac function and modulation of sarcomeric function by length. *Cardiovasc. Res.* 77:627–636. https://doi.org/10.1093/cvr/cvm099

Harris, S.P., C.R. Bartley, T.A. Hacker, K.S. McDonald, P.S. Douglas, M.L. Greaser, P.A. Powers, and R.L. Moss. 2002. Hypertrophic cardiomyopathy in cardiac myosin binding protein-C knockout mice. *Circ. Res.* 90:594–601. https://doi.org/10.1161/01.RES.0000012222.70819.64

Harris, S.P., B. Belknap, R.E. Van Sciver, H.D. White, and V.E. Galkin. 2016. C0 and C1 N-terminal Ig domains of myosin binding protein C exert different effects on thin filament activation. *Proc. Natl. Acad. Sci. USA.* 113:1558–1563. https://doi.org/10.1073/pnas.1518891113

Hofmann, P.A., M.L. Greaser, and R.L. Moss. 1991a. C-protein limits shortening velocity of rabbit skeletal muscle fibres at low levels of Ca^{2+} activation. *J. Physiol.* 439:701–715. https://doi.org/10.1113/jphysiol.1991.sp018689

Hofmann, P.A., H.C. Hartzell, and R.L. Moss. 1991b. Alterations in Ca^{2+} sensitive tension due to partial extraction of C-protein from rat skinned cardiac myocytes and rabbit skeletal muscle fibers. *J. Gen. Physiol.* 97:1141–1163. https://doi.org/10.1085/jgp.97.6.1141

Hooijman, P., M.A. Stewart, and R. Cooke. 2011. A new state of cardiac myosin with very slow ATP turnover: a potential cardioprotective mechanism in the heart. *Biophys. J.* 100:1969–1976. https://doi.org/10.1016/j.bpj.2011.02.061

Inchingolo, A.V., S.B. Previs, M.J. Previs, D.M. Warshaw, and N.M. Kad. 2019. Revealing the mechanism of how cardiac myosin-binding protein C N-terminal fragments sensitize thin filaments for myosin binding. *Proc. Natl. Acad. Sci. USA.* 116:6828–6835. https://doi.org/10.1073/pnas.1816480116

Iwamoto, H. 1998. Thin filament cooperativity as a major determinant of shortening velocity in skeletal muscle fibers. *Biophys. J.* 74:1452–1464. https://doi.org/10.1016/S0006-3495(98)77857-9

Jia, W., J.F. Shaffer, S.P. Harris, and J.A. Leary. 2010. Identification of novel protein kinase A phosphorylation sites in the M-domain of human and murine cardiac myosin binding protein-C using mass spectrometry analysis. *J. Proteome Res.* 9:1843–1853. https://doi.org/10.1021/pr901006h

Kampourakis, T., Z. Yan, M. Gautel, Y.B. Sun, and M. Irving. 2014. Myosin binding protein-C activates thin filaments and inhibits thick filaments in heart muscle cells. *Proc. Natl. Acad. Sci. USA.* 111:18763–18768. https://doi.org/10.1073/pnas.1413922112

Kampourakis, T., S. Ponnam, Y.B. Sun, I. Sevrieva, and M. Irving. 2018. Structural and functional effects of myosin-binding protein-C phosphorylation in heart muscle are not mimicked by serine-to-aspartate substitutions. *J. Biol. Chem.* 293:14270–14275. https://doi.org/10.1074/jbc.AC118.004816

Kensler, R.W., R. Craig, and R.L. Moss. 2017. Phosphorylation of cardiac myosin binding protein C releases myosin heads from the surface of cardiac thick filaments. *Proc. Natl. Acad. Sci. USA.* 114:E1355–E1364. https://doi.org/10.1073/pnas.1614020114

Lehrer, S.S. 1994. The regulatory switch of the muscle thin filament: Ca^{2+} or myosin heads? *J. Muscle Res. Cell Motil.* 15:232–236. https://doi.org/10.1007/BF00123476

Lu, Z., D.R. Swartz, J.M. Metzger, R.L. Moss, and J.W. Walker. 2001. Regulation of force development studied by photolysis of caged ADP in rabbit skinned psoas fibers. *Biophys. J.* 81:334–344. https://doi.org/10.1016/S0006-3495(01)75703-7

Mamidi, R., K.S. Gresham, J. Li, and J.E. Stelzer. 2017. Cardiac myosin binding protein-C Ser^{302} phosphorylation regulates cardiac β-adrenergic reserve. *Sci. Adv.* 3:e1602445. https://doi.org/10.1126/sciadv.1602445

Martyn, D.A., P.B. Chase, J.D. Hannon, L.L. Huntsman, M.J. Kushmerick, and A.M. Gordon. 1994. Unloaded shortening of skinned muscle fibers from rabbit activated with and without Ca^{2+} *Biophys. J.* 67:1984–1993. https://doi.org/10.1016/S0006-3495(94)80681-2

McKillop, D.F.A., and M.A. Geeves. 1993. Regulation of the interaction between actin and myosin subfragment 1: evidence for three states of the thin filament. *Biophys. J.* 65:693–701. https://doi.org/10.1016/S0006-3495(93)81110-X

McNamara, J.W., A. Li, N.J. Smith, S. Lal, R.M. Graham, K.B. Kooiker, S.J. van Dijk, C.G.D. Remedios, S.P. Harris, and R. Cooke. 2016. Ablation of cardiac myosin binding protein-C disrupts the super-relaxed state of myosin in murine cardiomyocytes. *J. Mol. Cell. Cardiol.* 94:65–71. https://doi.org/10.1016/j.yjmcc.2016.03.009

McNamara, J.W., R.R. Singh, and S. Sadayappan. 2019. Cardiac myosin binding protein-C phosphorylation regulates the super-relaxed state of myosin. *Proc. Natl. Acad. Sci. USA.* 116:11731–11736. https://doi.org/10.1073/pnas.1821660116

Morris, C.A., L.S. Tobacman, and E. Homsher. 2003. Thin filament activation and unloaded shortening velocity of rabbit skinned muscle fibres. *J. Physiol.* 550:205–215. https://doi.org/10.1113/jphysiol.2003.040899

Moss, R.L. 1986. Effects on shortening velocity of rabbit skeletal muscle due to variations in the level of thin-filament activation. *J. Physiol.* 377:487–505. https://doi.org/10.1113/jphysiol.1986.sp016199

Mun, J.Y., M.J. Previs, H.Y. Yu, J. Gulick, L.S. Tobacman, S. Beck Previs, J. Robbins, D.M. Warshaw, and R. Craig. 2014. Myosin-binding protein C displaces tropomyosin to activate cardiac thin filaments and governs their speed by an independent mechanism. *Proc. Natl. Acad. Sci. USA.* 111:2170–2175. https://doi.org/10.1073/pnas.1316001111

Patel, J.R., J.M. Pleitner, R.L. Moss, and M.L. Greaser. 2012. Magnitude of length-dependent changes in contractile properties varies with titin isoform in rat ventricles. *Am. J. Physiol. Heart Circ. Physiol.* 302:H697–H708. https://doi.org/10.1152/ajpheart.00800.2011

Patel, J.R., G.P. Barton, R.K. Braun, K.N. Goss, K. Haraldsdottir, A. Hopp, G. Diffee, T.A. Hacker, R.L. Moss, and M.W. Eldridge. 2017. Altered right ventricular mechanical properties are afterload dependent in a rodent model of bronchopulmonary dysplasia. *Front. Physiol.* 8:840. https://doi.org/10.3389/fphys.2017.00840

Pi, Y., K.R. Kemnitz, D. Zhang, E.G. Kranias, and J.W. Walker. 2002. Phosphorylation of troponin I controls cardiac twitch dynamics: evidence from phosphorylation site mutants expressed on a troponin I-null background in mice. *Circ. Res.* 90:649–656. https://doi.org/10.1161/01.RES.0000014080.82861.5F

Previs, M.J., S. Beck Previs, J. Gulick, J. Robbins, and D.M. Warshaw. 2012. Molecular mechanics of cardiac myosin-binding protein C in native thick filaments. *Science.* 337:1215–1218. https://doi.org/10.1126/science.1223602

Previs, M.J., J.Y. Mun, A.J. Michalek, S.B. Previs, J. Gulick, J. Robbins, D.M. Warshaw, and R. Craig. 2016. Phosphorylation and calcium antagonistically tune myosin-binding protein C's structure and function. *Proc. Natl. Acad. Sci. USA.* 113:3239–3244. https://doi.org/10.1073/pnas.1522236113

Risi, C., B. Belknap, E. Forgacs-Lonart, S.P. Harris, G.F. Schröder, H.D. White, and V.E. Galkin. 2018. N-terminal domains of cardiac myosin binding protein C cooperatively activate the thin filament. *Structure.* 26:1604–1611.e4. https://doi.org/10.1016/j.str.2018.08.007

Rosas, P.C., Y. Liu, M.I. Abdalla, C.M. Thomas, D.T. Kidwell, G.F. Dusio, D. Mukhopadhyay, R. Kumar, K.M. Baker, B.M. Mitchell, et al. 2015. Phosphorylation of cardiac Myosin-binding protein-C is a critical mediator of diastolic function. *Circ. Heart Fail.* 8:582–594. https://doi.org/10.1161/CIRCHEARTFAILURE.114.001550

Sadayappan, S., J. Gulick, H. Osinska, D. Barefield, F. Cuello, M. Avkiran, V.M. Lasko, J.N. Lorenz, M. Maillet, J.L. Martin, et al. 2011. A critical function for Ser-282 in cardiac Myosin binding protein-C phosphorylation and cardiac function. *Circ. Res.* 109:141–150. https://doi.org/10.1161/CIRCRESAHA.111.242560

Stelzer, J.E., J.R. Patel, and R.L. Moss. 2006. Protein kinase A-mediated acceleration of the stretch activation response in murine skinned myocardium is eliminated by ablation of cMyBP-C. *Circ. Res.* 99:884–890. https://doi.org/10.1161/01.RES.0000245191.34690.66

Strang, K.T., N.K. Sweitzer, M.L. Greaser, and R.L. Moss. 1994. β-adrenergic receptor stimulation increases unloaded shortening velocity of skinned single ventricular myocytes from rats. *Circ. Res.* 74:542–549. https://doi.org/10.1161/01.RES.74.3.542

Swartz, D.R., and R.L. Moss. 2001. Strong binding of myosin increases shortening velocity of rabbit skinned skeletal muscle fibres at low levels of Ca^{2+}. *J. Physiol.* 533:357–365. https://doi.org/10.1111/j.1469-7793.2001.0357a.x

Swartz, D.R., R.L. Moss, and M.L. Greaser. 1996. Calcium alone does not fully activate the thin filament for S1 binding to rigor myofibrils. *Biophys. J.* 71:1891–1904. https://doi.org/10.1016/S0006-3495(96)79388-8

Tong, C.W., J.E. Stelzer, M.L. Greaser, P.A. Powers, and R.L. Moss. 2008. Acceleration of crossbridge kinetics by protein kinase A phosphorylation of cardiac myosin binding protein C modulates cardiac function. *Circ. Res.* 103:974–982. https://doi.org/10.1161/CIRCRESAHA.108.177683

Tong, C.W., X. Wu, Y. Liu, P.C. Rosas, S. Sadayappan, A. Hudmon, M. Muthuchamy, P.A. Powers, H.H. Valdivia, and R.L. Moss. 2015. Phosphoregulation of cardiac inotropy via myosin binding protein-C during increased pacing frequency of β_1-adrenergic stimulation. *Circ. Heart Fail.* 8:595–604. https://doi.org/10.1161/CIRCHEARTFAILURE.114.001585

van Dijk, S.J., K.L. Bezold, and S.P. Harris. 2014. Earning stripes: myosin binding protein-C interactions with actin. *Pflugers Arch.* 466:445–450. https://doi.org/10.1007/s00424-013-1432-8

Weith, A., S. Sadayappan, J. Gulick, M.J. Previs, P. Vanburen, J. Robbins, and D.M. Warshaw. 2012. Unique single molecule binding of cardiac myosin binding protein-C to actin and phosphorylation-dependent inhibition of actomyosin motility requires 17 amino acids of the motif domain. *J. Mol. Cell. Cardiol.* 52:219–227. https://doi.org/10.1016/j.yjmcc.2011.09.019